

Predicting Glass-to-Glass and Liquid-to-Liquid Phase Transitions in Water

Robert F. Tournier^{1,2}

¹*Univ. Grenoble Alpes, Inst. NEEL, F-38042 Grenoble Cedex 9, France*

²*CNRS, Inst. NEEL, F-38042 Grenoble, France*

E-mail address: robert.tournier@neel.cnrs.fr

Abstract: Glass-to-glass and liquid-to-liquid phase transitions are observed in bulk and confined supercooled water, with or without applied pressure. They result from the competition of two liquid phases separated by an enthalpy difference depending on temperature. The classical nucleation equation of these phases is completed by this quantity existing at all temperatures, a pressure contribution, and an enthalpy excess. The thermodynamic parameters of amorphous water, the double glass transition temperatures, and enthalpy and volume changes are predicted in agreement with experimental results. These sharp transitions to ultrastable polyamorphous bulk phases open the way to discover new ultrastable glasses.

Introduction: Multiple liquid-to-liquid phase transitions (LLPTs) observed in several metallic glass-forming melts have already been predicted using a classical nucleation equation completed by an enthalpy difference of two liquid phases depending on the square of the reduced temperature $\theta = (T - T_m)/T_m$, T_m as the melting temperature [1]. The objectives of this paper are to extend the application of this renewed equation to the thermodynamic properties of water, to explain the occurrence of glass-to-glass phase transitions in amorphous water, and to show that the high-density phases obtained under pressure are ultrastable glass phases analogous to those produced by vapor deposition at temperatures close to T_g [2-5].

Any glass relaxes enthalpy below T_g . The density of amorphous water decreases during relaxation. The quasi-equilibrium of density and enthalpy is far from being obtained by relaxation. First-order transformations under pressure are observed in amorphous water bulk samples [6-12], because the pressure adds an enthalpy contribution and facilitates the glass transformation towards an equilibrium phase. Any glass freezes enthalpy and entropy at T_g , which are available for exothermic relaxation. This relaxed entropy and enthalpy cannot exceed the value of the frozen enthalpy and entropy [13].

The water glass state is obtained by vapor deposition, liquid hyperquenching, confined water cooling, and high pressure applied to ice [14]. A warm-up of bulk amorphous water produces an endothermic event just below the crystallization temperature, occurring at around 136 K [15-17]. The glass transition is characterized by a specific heat jump preceding the occurrence of crystallization [17]. Applying high pressure to ice reduces T_m and produces liquid and amorphous water. Sharp transformations viewed as first-order transitions are observed under pressure at 77 K, and at higher temperatures. These findings show that a bulk amorphous liquid having low density can be transformed under pressure into high-density amorphous liquid [8,11,17]. Three glass states have been identified under pressure: low density amorphous liquid (LDA); high density amorphous liquid (HDA); and very high density amorphous liquid (VHDA). Transformations of LDA to HDA and VHDA are observed after increasing pressure up to 16 kbar, and decompression down to residual pressures p at temperatures smaller than T_g . Some VHDA,

HDA and LDA are studied after complete decompression down to 77 K [2,12]. HDA obtained after decompression at 77 K down to 100 bar is also transformed by heating at ~140K in LDA [10]. The HDA phase is recovered by a new compression at $p=0.32\text{GPa}$.

Measurements of water confined within silica gel in 1.1nm pores show the existence of a broad and high specific heat peak at 227.5K (-45.6°C), and two heat flow changes at 130–143 and 160–190 K, showing the presence of two glass transitions [19,20]. A pronounced minimum of compressibility is still observed in water at a temperature of +45.5°C, which is symmetrical with regard to T_m at ambient pressure of the transition at -45.6°C [21,22]. A specific heat increase below 273 K is still observed in bulk supercooled water at ambient pressure down to the crystallization temperature [14,23], confirming the existence, in the absence of crystallization, of a liquid-to-liquid phase transition (LLTP) at 227.5K [20,24].

These phenomena are attributed, in the first model of two liquids, to the existence of a critical point leading to a line of first-order LLPTs [22,25-28]. The two liquids have the same chemical composition and contain low- and high-density species forming differently bonded domains. Such LLPTs form part of the general phenomenology for a wide range of liquids [29]. These ideas are successful to explain the existence of LLPTs, but are not able to predict glass thermodynamic properties, because they view them as a result of freezing, instead of a thermodynamic transition related to the difference of enthalpy of Phase 1 and Phase 2. Supercooled water undergoes a LLPT at 227.5 K, which looks like a first-order transformation of strong glass to fragile liquid [26].

In this paper, the classical nucleation equation is completed by introducing the enthalpy changes $\varepsilon_{ls}\times\Delta H_m$, $\varepsilon_{gs}\times\Delta H_m$, and $\Delta\varepsilon_{lg}\times\Delta H_m$, respectively, associated with growth critical nucleus formation leading to Phase 1 and Phase 2 above T_g and Phase 3 below T_g , where ΔH_m is the melting heat [30]. The enthalpy difference $\Delta\varepsilon_{lg}\times\Delta H_m$, associated with the formation of vitreous Phase 3 below T_g , is then equal to $(\varepsilon_{ls}-\varepsilon_{gs})\times\Delta H_m$. The coefficients ε_{ls} and ε_{gs} are linear functions of $\theta^2=(T-T_m)^2/T_m^2$, as shown by studying supercooling rate maxima of liquid elements [31]. A positive sign of $\Delta\varepsilon_{lg}=(\varepsilon_{ls}-\varepsilon_{gs})$ above T_g and T_m at a reduced temperature θ shows that Phase 1 is favored; a negative value reveals that it is Phase 2 [1]. The first-order transition to a glass of confined liquid helium under pressure has been described using $\varepsilon_{ls0}=\varepsilon_{gs0}=0.217$ [32]. This glass is ultrastable because there is no more enthalpy to relax in this state. These values of ε_{ls0} and ε_{gs0} , determined in many pure liquid elements at their melting temperature T_m , correspond to the Lindemann coefficient 0.103 [33]. The transformation temperature T_{sg} of glasses in ultrastable phases with higher density has been defined as a function of a frozen enthalpy excess $\Delta\varepsilon\times\Delta H_m$. The denser ultrastable glass attains its lowest enthalpy at a transformation temperature T_{sg} for $\Delta\varepsilon=(\varepsilon_{ls0}-\varepsilon_{gs0})$, above which there is no more enthalpy to relax [5]. The transformation of Phase 3 into polyamorphous ultrastable phases under pressure produces sharp enthalpy changes that are predicted by this model.

2-Basic equations applied to water

The nucleation equation is given by (1):

$$\Delta G = \frac{4\pi R^3}{3} \Delta H_m / V_m \times (\theta - \varepsilon) + 4\pi R^2 (1 + \varepsilon) \sigma_1 \Delta H_m / V_m \quad (1)$$

where ΔG is the Gibbs free energy change associated with the formation of a spherical growth nucleus of radius R , ε is a fraction of the melting enthalpy ΔH_m , V_m the molar volume, and $\theta=(T-T_m)/T_m$ the reduced temperature. The melting heat ΔH_m and T_m are assumed to be the same whatever the nucleus radius R is, and do not depend on the Laplace pressure. The critical nucleus can give rise to Phase 1 or Phase 2, or amorphous Phase 3, or various LLPT, according to values ε_{ls} , ε_{gs} and $\Delta\varepsilon_{lg}$ of the coefficient ε . The new surface energy is $(1+\varepsilon)\times\sigma_1$ instead of σ_1 . The classical equation is obtained for $\varepsilon=0$ [34]. The homogeneous nucleation temperatures are $\theta_{n-}=(\varepsilon-2)/3$ for $\theta < 0$ and $\theta_{n+}=\varepsilon$ for $\theta > 0$ [1,30]. The critical radius is infinite at the homogeneous nucleation temperature obtained for $\theta=\varepsilon$ instead of $\theta=0$ for the classical equation. A catastrophe of nucleation occurs at $\theta=\varepsilon$ for crystals protected against surface melting [35].

The coefficients ε_{ls} and ε_{gs} in (2) and (3) are values of $\varepsilon(\theta)$, respectively, leading to a nucleus formation having the critical radius for Phase 1 and Phase 2 formations under pressure:

$$\varepsilon_{ls}(\theta) = \varepsilon_{ls0}(1 - \theta^2 \times \theta_{0m}^{-2}) + \Delta\varepsilon + P_1, \quad (2)$$

$$\varepsilon_{gs}(\theta) = \varepsilon_{gs0}(1 - \theta^2 \times \theta_{0g}^{-2}) + P_2, \quad (3)$$

where $\Delta\varepsilon$ is the coefficient of enthalpy excess being frozen after quenching the melt, $P_1=(p-p_0)\times V_{m1}/\Delta H_m$ and $P_2=(p-p_0)\times V_{m2}/\Delta H_m$ are the contributions of the pressure p to the enthalpy coefficients ε_{ls} and ε_{gs} , and p_0 is the ambient pressure [5]. The coefficients ε_{ls} and ε_{gs} are equal to zero at the reduced temperatures θ_{0m} and θ_{0g} for $\Delta\varepsilon=0$ and $P_1=0$, and correspond to the Vogel-Fulcher-Tammann temperatures above and below T_g , respectively. Equations (2) and (3) are respected at the homogeneous nucleation temperatures θ_{n-} in Phase 1 and Phase 2. Equation (4) determines θ_{n-} of Phase 2 combining (3) with $\theta_{n-}=(\varepsilon_{gs}-2)/3$ [30]:

$$\theta_{n-}^2 \times \varepsilon_{gs0} \times \theta_{0g}^{-2} + 3\theta_{n-} + 2 - \varepsilon_{gs0} - P_2 = 0 \quad (4)$$

The solutions for θ_{n-} are given by (5):

$$\theta_{n-} = (-3 \pm [9 - 4(2 - \varepsilon_{gs0} - P_2)\varepsilon_{gs0} / \theta_{0g}^2]^{1/2})\theta_{0g}^2 / (2\varepsilon_{gs0}) \quad (5)$$

θ_{n-} of Phase 2 for the sign + is called θ_2 , given by (5).

Equation (6) determines the homogeneous nucleation temperature θ_{n-} of Phase 1 combining (2) at this temperature with $\theta_{n-}=(\varepsilon_{ls}-2)/3$:

$$\theta_{n-}^2 \times \varepsilon_{ls0} \times \theta_{0m}^{-2} + 3\theta_{n-} + 2 - \varepsilon_{ls0} - \Delta\varepsilon - P_1 = 0 \quad (6)$$

The reduced homogeneous nucleation temperature θ_{n-} of Phase 1 under pressure in (7) is deduced from (6):

$$\theta_{n-} = (-3 \pm [9 - 4(2 - \varepsilon_{ls0} - \Delta\varepsilon - P_1)\varepsilon_{ls0} / \theta_{0m}^2]^{1/2})\theta_{0m}^2 / (2\varepsilon_{ls0}) \quad (7)$$

θ_n in (7) is called θ_1 for the sign +. The glass transition occurs at θ_g when $\varepsilon_{ls}(\theta)$ in (2) is equal to $\varepsilon_{gs}(\theta)$ in (3). θ_1 and θ_2 are equal to θ_g in strong glasses because $\varepsilon_{ls}(\theta_g)=\varepsilon_{gs}(\theta_g)$ for $\Delta\varepsilon=0$ and $P_1=P_2=0$.

As water is a strong glass at low temperatures, the coefficients ε_{gs0} in (8) and ε_{ls0} in (9), deduced from (4) with $P_2=0$ and from (6) with $P_1=0$ and $\Delta\varepsilon=0$, are determined from the knowledge of θ_g , θ_{0g} , and θ_{0m} [30]:

$$\varepsilon_{gs0} = \frac{3\theta_g + 2}{1 - \theta_g^2 / \theta_{0g}^2} \quad (8)$$

$$\varepsilon_{ls0} = \frac{3\theta_g + 2}{1 - \theta_g^2 / \theta_{0m}^2} \quad (9)$$

where the reduced temperatures θ_{0g} and θ_{0m} are equal to -1 and -2/3, respectively, because the Vogel-Fulcher Tamman temperatures are equal to 0 K below T_g and to $T_m/3$ above T_g for many pure strong liquid elements [31]. With $T_g=136.6$ K, $\theta_g=-0.5$, ε_{gs0} is equal to 0.66667 and ε_{ls0} to 1.14286. The frozen enthalpy at T_g is equal to the minimum value $-0.37037 \times \Delta H_m$ of $(\varepsilon_{ls} - \varepsilon_{gs}) \times \Delta H_m$ obtained for $\varepsilon_{ls}=0$ at $\theta=\theta_{0m}=-2/3$. The heat capacity jump at T_g is equal to: $(d\varepsilon_{ls}/dT - d\varepsilon_{gs}/dT) \times \Delta H_m = -1.905 \times \Delta H_m / T_m = 41.9 \text{ JK}^{-1} \text{ mole}^{-1}$ in agreement with old measurements [17], as shown in Figure 1.

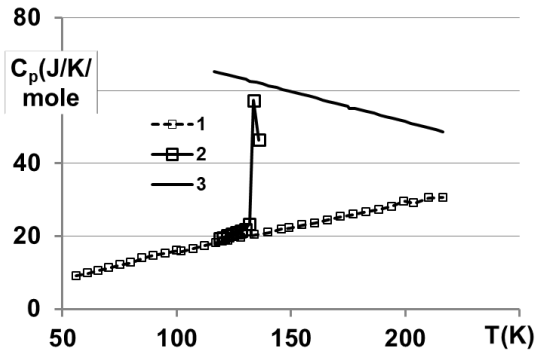


Figure 1: 1. Heat capacity of hexagonal ice [10]; 2. Heat capacity jump at 133.6 K [10]; 3. Supercooled water heat capacity calculated with the derivative $(d\varepsilon_{ls}/dT - d\varepsilon_{gs}/dT) \times \Delta H_m$.

For confined supercooled water in pores of radius $R=0.55$ nm [19,20], θ_2 is equal at the critical point to -0.16715 (227.5K) for $P_2=0.8505$ in (5). Using the Young-Laplace equation, Δp is equal to $2\gamma/R=0.31 \pm 0.02$ GPa, with a value of the surface tension $\gamma=0.085 \pm 0.005 \text{ J/m}^2$ at 227.5K extrapolated from its thermal variation above 250K [23]. The enthalpy coefficient P_2 is deduced to be close to 0.8505 with $V_{m2} \cong 16.5 \times 10^{-6} \text{ m}^3$ and $p=0.31$ GPa.

The enthalpy difference coefficient $\Delta\varepsilon_{lg}$ associated with vitreous Phase 3 is given by (9) under pressure p :

$$\Delta\varepsilon_{lg}(\theta) = (\varepsilon_{ls} - \varepsilon_{gs}) = \varepsilon_{ls0} - \varepsilon_{gs0} + \Delta\varepsilon + P_1 - P_2 - \theta^2 \left(\frac{\varepsilon_{ls0}}{\theta_{0m}^2} - \frac{\varepsilon_{gs0}}{\theta_{0g}^2} \right) \quad (9)$$

The difference $\Delta P=(P_1-P_2)=\delta V \times p/\Delta H_m$ is proportional to the volume change δV , and to the pressure p at the transformation temperature θ . ΔP is equal to zero for $\delta V=0$ in the absence of latent heat. The homogeneous nucleation temperature of Phase 3 also occurs for $\Delta \varepsilon_{lg}=0$ with $\Delta \varepsilon=0$ because Phase 1 and Phase 2 have the same homogeneous nucleation temperature $\theta_1=\theta_2=\theta_g$.

A sharp enthalpy difference between nonrelaxed Phase 3 and fully relaxed Phase 3 can be induced in all glasses below T_g for $\Delta \varepsilon_{lg}=0$ in (9), when an enthalpy excess coefficient $\Delta \varepsilon$ exists after rapid cooling, as already described for an ultrastable glass formation [5]. This enthalpy difference is equal to $2 \times \Delta \varepsilon_{lg}(\theta) \times \Delta H_m$ because the enthalpy of the ultrastable phase cannot exceed that of the available enthalpy at any temperature. This transformation temperature T_{sg} for a stable glass formation given in (10) is induced by pressure. It depends on δV and on the value of $\Delta \varepsilon$ at this temperature.

$$\theta_{sg} = - \left[(\varepsilon_{ls0} - \varepsilon_{gs0} + \Delta \varepsilon + \Delta P) / (\varepsilon_{ls0} \theta_{0m}^{-2} - \varepsilon_{gs0} \theta_{0g}^{-2}) \right]^{1/2} \quad (10)$$

Such sharp transitions are observed after complete decompression of VHDA at 77K from various pressures, and are reproduced in Figure 2 [36].

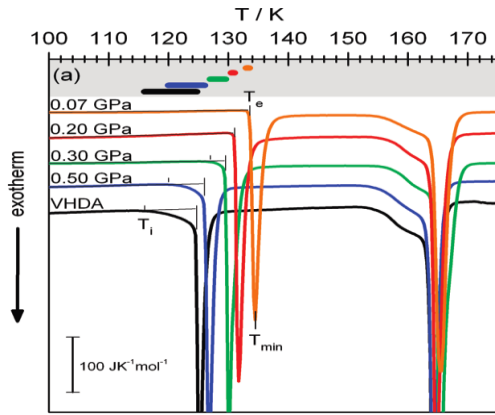


Figure 2: Reprinted from [36, Figure 3]. “DSC scans recorded at a rate of 10 K/min. The DSC output signal was normalized to 1 mol. The samples were heated from 93 to 253 K; thermograms are plotted in the temperature range of 100–175 K. Shown are VHDA (black line) and four samples made by decompression of VHDA at 140 K to 0.5 (blue line), 0.3 (green line), 0.2 (red line), and 0.07 GPa (orange line). First exothermic peak: transition to LDA; second exothermic peak: crystallization to cubic ice. The bars in the top part indicate the difference between T_i and T_e , which is a measure of the relaxation state of the sample.” There is no detectable endothermal event at $T=136.6K$.

Several lines of $\Delta \varepsilon_{lg}$ given by (9) are represented in Figure 3. The line $\Delta \varepsilon_{lg}=0$ is plotted versus θ for $P_1-P_2=0$ and $\Delta \varepsilon=1.14286 \times (1-2.25 \times \theta^2)-0.66667 \times (1-\theta^2)$. This corresponds to the lowest density of the LDA phase. The coefficient $\Delta \varepsilon$ sharply disappears at $\theta=\theta_{sg}$, seen as a first “ T_g ”. Line 1 corresponds to the nonrelaxed glass Phase 3, with $\Delta \varepsilon_{lg}$ given by (9) for $\Delta \varepsilon=0$ and $P_1-P_2=0$. Line 2 represents $\Delta \varepsilon_{lg}$ of the ultrastable glass of Phase 3 above θ_{sg} . This $\Delta \varepsilon_{lg}$ is equal to $2 \times 0.37037 \times (T_{sg}-T_g)/(T_g-91)=0.00407 \times (T_{sg}-136.6)$. The available latent heats $\Delta \varepsilon_{lg} \times \Delta H_m$ along Line 2 are in rough agreement with those observed in Figure 2.

The true $T_g=136.6\text{K}$ without applied pressure is expected for the transformation of Phase 3 into Phase 1. On Line 3 of Figure 3, the first T_g of confined water in 1.1nm pores is 115K, whereas the true T_g is 162K. Several other examples of double transition are presented in Figure 3 and correspond to those of Figure 2.

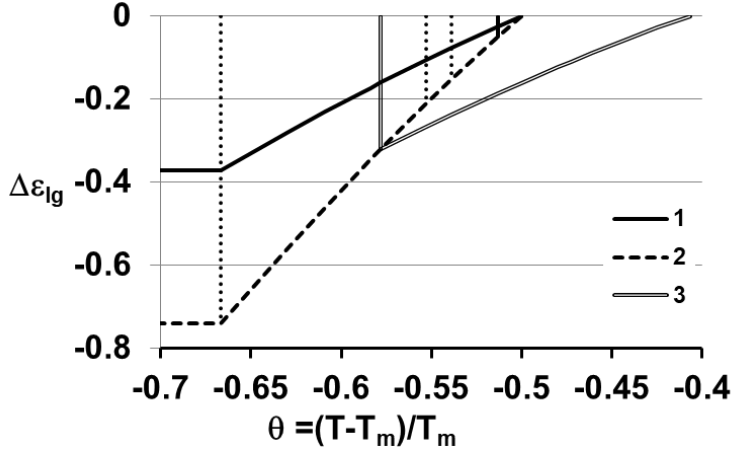


Figure 3: *Reduced temperatures θ_{sg} along the line $\Delta\epsilon_{lg}=0$ and latent heat coefficients $\Delta\epsilon_{lg}$ associated with the glass-to-glass transformations after decompression. Curves numbered from 1 to 4: 1. $\Delta\epsilon_{lg}(\theta)$ given by (9) of nonrelaxed Phase 3 with $\Delta\epsilon=0$, $\Delta P=0$, $\theta_g=-0.5$ ($T_g=136.6\text{K}$); 2. Equilibrium enthalpy coefficient $2\times\Delta\epsilon_{lg}(\theta)$ of ultrastable Phase 3 crossing $\theta_g=-0.5$ ($T_g=136.6\text{K}$) without endothermal event; 3. $\Delta\epsilon_{lg}(\theta)$ starting after transition from $\theta_{sg}=-0.578$, $T_{sg}=115.3\text{K}$ with $\Delta\epsilon=0$ and $\Delta P=-0.1608$, corresponding to the Laplace pressure at 162K in 1.1nm pores [19] and finishing at $\theta_g=-0.4069$, $T_g=162\text{K}$. Other reduced temperatures θ_{sg} equal to -0.66667, -0.55277, -0.5387, and -0.51307, corresponding to $T_s=91$, 122.2, 126, and 133K, respectively.*

The glass transition at 136.6K is not detected, as shown in Figure 2. Then, the transitions at T_{sg} give rise to amorphous ice instead of fully relaxed Phase 3. The latent heat at its crystallization temperature at 164K would have to depend on the exothermic heat recovered at T_{sg} . This analysis confirms recent findings that the sharp transitions of polymorphous LDA phases at $p=0$ [36] lead to amorphous ice resulting from molecular reorientation processes [37]. The enthalpy coefficient along Line 2 in Figure 3 cannot be attained by Phase 3, because the weakest density of Phase 3 would be smaller than that of ice. The glass phase is recovered in relaxed samples because their density is higher along Line 1 [37]. The latent heat only appear above 125K instead of $T_m/3=91\text{K}$ as shown in Figure 2. A limiting factor could be the available entropy below T_g . The VHDA phases prepared from very high pressures do not lead, after complete decompression, to higher density phases in the range 120–135K than those obtained applying lower pressures.

There are two regions of crystallization of water around 230–250K and 135–165K. Supercooled water undergoes a first-order phase transition that separates fragile from strong states. Fragile liquids have maximized values of ϵ_{ls0} and ϵ_{gs0} :

$$\epsilon_{ls}(\theta=0) = \epsilon_{ls0} + P_1 = 1.5 \times \theta_1 + 2 + P_1 = a \times \theta_g + 2 + P_1, \quad (11)$$

where a is defined by the specific heat excess $\Delta C_p(T)$ of the supercooled melt at the glass transition [38-40]. For $a < 1$, the glass transition has a first-order character [30]. The reduced temperature θ_{0m} is given by (12), and is a double solution for (6):

$$\theta_{0m}^2 = \frac{8}{9} \varepsilon_{ls0} - \frac{4}{9} \varepsilon_{ls0} (\varepsilon_{ls0} + P_1). \quad (12)$$

New parameters ε_{gs0} and θ_{0g} are fixed at T_g and below T_g by (13) and (14), to have a double solution for (4):

$$\varepsilon_{gs}(\theta = 0) = \varepsilon_{gs0} + P_2 = 1.5 \times \theta_g + 2 + P_2, \quad (13)$$

$$\theta_{0g}^2 = \frac{8}{9} \varepsilon_{gs0} - \frac{4}{9} \varepsilon_{gs0} (\varepsilon_{gs0} + P_2). \quad (14)$$

The LLPT in fragile water occurs at 227.5K ($\theta_{LL} = -0.16715$) [19]. This temperature does not depend on pressure because it occurs when $\Delta\varepsilon_{lg}$ is equal to 0 in (9), with $\Delta\varepsilon = 0$ and $P_1 = P$, and because $\Delta\varepsilon_{lg} = 0$ is still reproduced in (9) at the isothermal compressibility minimum temperature $\theta_{LL} = -0.16715$, $T_{LL} = 318.8K$, P_1 and $P_2 = 0$, $\Delta\varepsilon = 0$ [22,41,42]. The fragile water specific heat excess would have to be equal to 109.3J/mole with $a = 0.55$ at a virtual first-order glass transition $\theta_g = -0.276$ in the absence of an LLPT, with the following parameters: $\varepsilon_{ls0} = 1.8482$, $\varepsilon_{gs0} = 1.586$, $\theta_{0m}^2 = 0.12469$, and $\theta_{0g}^2 = 0.29182$, shown in Figure 4. Under these conditions, the water specific heat excess could increase up to 81 J/mole at $\theta_{LL} = -0.16715$ [19] assuming a linear variation from $\theta = 0$ ($\Delta C_p = 37$ J/mole) to $\theta = -0.276$ ($\Delta C_p = 109.3$ J/mole) in the absence of LLPT. This specific heat increase is not only observed at zero pressure [46-45], but also under a Laplace pressure of 0.31 ± 0.02 GPa in 1.1 nm pores, slightly increasing with decreasing temperature. In Figure 4, the LLPT at 227.5K is accompanied during heating by an endothermal latent heat of $0.364 \times \Delta H_m$.

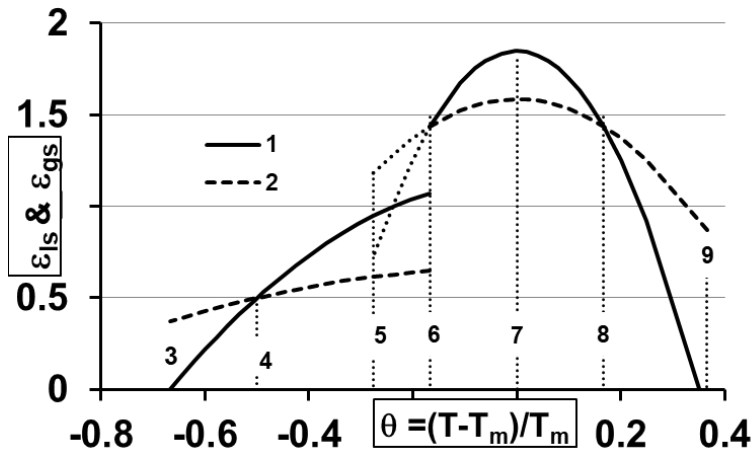


Figure 4: The enthalpy coefficients ε_{ls} and ε_{gs} versus θ of Phase 1 and Phase 2: curves numbered from 1 to 2: 1. $\varepsilon_{ls}(\theta)$ given by (2) below $\theta_{LL} = -0.167$ in the strong water and above in the fragile one; 2. $\varepsilon_{gs}(\theta)$ given by (3) below $\theta_{LL} = -0.167$ and above temperatures numbered from 3 to 9: 3. The frozen enthalpy

coefficient $\Delta\varepsilon_{ig}$ equal to -0.37037 at $\theta=-2/3$; 4. The strong water transition $\theta_g=-0.5$ ($T_g=136.6$ K); 5. $\theta_g=-0.276$ of the fragile water in the absence of LLTP; 6. At $\theta_{LL}=-0.167$, $T_{LL}=227.5$ K, the LLTP for $\Delta\varepsilon_{ig}=0$ and a latent heat $0.364 \times \Delta H_m$; 7. $\theta=0$ the melting temperature at $T_m=273.14$ K; 8. For $\theta=0.167$, $\Delta\varepsilon_{ig}=0$ at the isothermal compressibility minimum temperature 318.7 K; 9. $\theta=0.366$, the boiling temperature.

2- Transformation of LDA to ultrastable HDA under pressure

High pressure applied to ice samples followed by complete decompression induces an LDA phase [11]. In all experiments involving high pressures applied below $T_g=136.6$ K, some enthalpy excess $\Delta\varepsilon$ is frozen because the melting temperature T_m is strongly decreased, and the sample is cooled during decompression from temperatures much larger than T_m . Compression experiments of this LDA phase at various temperatures transform it into an HDA phase at a well-defined pressure p , inducing a sharp transition. The volume change δV does not depend on the pressure p and is equal to 0.22×10^{-6} m³/g, as shown in Figure 5 [9].

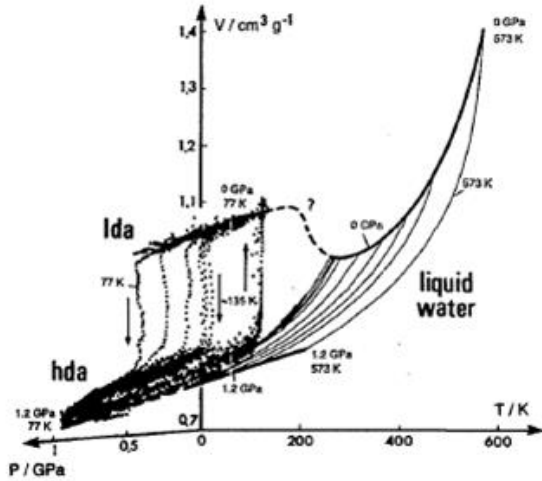


Figure 5: Specific volume versus pressure (GPa) and Temperature (K). “Low density amorphous to high density amorphous transformations under pressure occur for $p=0.55, 0.45, 0.38, 0.32, 0.05$ GPa and $T=77, 100, 121, 135, 135$ K respectively. Liquid water under 1.2 GPa and 0 pressures is also represented versus temperature. The linkage between LDA and liquid state at zero pressure occurs at 227 K. The liquid at zero pressure corresponds to Phase 1” Reprinted from [9, Figure 4].

The equilibrium enthalpy change under pressure from LDA to HDA phase is equal to $\Delta P=p \times \delta V / \Delta H_m$. Fully relaxed Phase 3 (HDA) is expected to have a maximum enthalpy difference with nonrelaxed Phase 3 (LDA) equal to $-0.37037 \times \Delta H_m$, as shown by the difference between Line 1 and Line 2 in Figure 3. In Figure 6, the enthalpy coefficient changes $\Delta\varepsilon_{ig}$ are represented as a function of the reduced temperatures θ calculated from (10). The values of $\Delta\varepsilon$ and ΔP are indicated in the Figure 4 caption. Those of $\Delta\varepsilon$ decrease with temperature and disappear around 136.6 K, as already observed in ethylbenzene [5,46]. Those of ΔP are proportional to the pressure p . The maximum value $\Delta\varepsilon_{ig}=-0.37037$ is obtained for all pressures $p \leq 0.55$ GPa. Then, the HDA phase corresponds to the largest enthalpy change associated with

the formation of an ultrastable glass phase. The calculated volume change $0.224 \times 10^{-6} \text{m}^3/\text{g}$ is constant under various pressures p , and equal to the experimental value. The chosen values of T_m under pressure are those of hexagonal ice [8]. The highest density of the HDA phase is obtained at 77K. The polyamorphous ultrastable glass phase becomes less dense at higher temperatures T_{sg} . The LDA-to-HDA transformation occurring for $p=0.32\text{GPa}$ in the interval 130–140K is reversible when the pressure is decreased down to $p=0.05\text{GPa}$. The glass transition falls from 150.6K to 139.6K when p is reduced, whereas the LDA phase is recovered. This reversibility tends to prove the first-order character of the transition. The enthalpy excess $\Delta\varepsilon \times \Delta H_m$ of LDA is fully recovered at $T=T_{sg}$ and $p=0$ instead of being relaxed, because the LDA phase density cannot be smaller than that of ice. The effect of pressure is to decrease the enthalpy and the volume by a constant quantity without relaxing $\Delta\varepsilon \times \Delta H_m$. It is only relaxed at $p=0$ decreasing the volume and leading to amorphous ice, as shown in Figure 2.

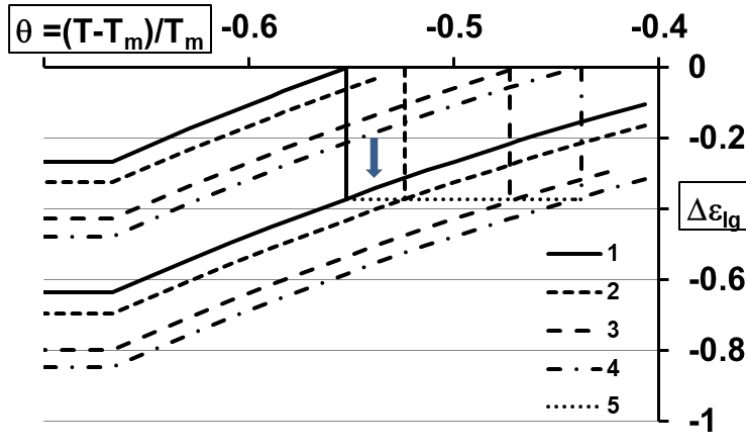


Figure 6: Calculated reduced temperatures θ_{sg} of low density amorphous (LDA)-to-high density amorphous (HDA) transformations under constant pressure p using (10) in agreement with experiments shown in Figure 5. Curves numbered from 1 to 5: 1. $\Delta\varepsilon_{lg}(\theta)$ for $\Delta\varepsilon = \varepsilon_{lso} - \varepsilon_{gs0} = 0.47619$, $\Delta P = -0.37037$, $p = 0.55\text{GPa}$, $T_m = 172\text{K}$, $\theta_{sg} = -0.55278$, $T_{sg} = 77\text{K}$; 2. $\Delta\varepsilon_{lg}(\theta)$ for $\Delta\varepsilon = 0.349$, $\Delta P = -0.30103$, $p = 0.45\text{GPa}$, $T_m = 210\text{K}$, $\theta_{sg} = -0.52357$, $T_{sg} = 100\text{K}$; 3. $\Delta\varepsilon_{lg}(\theta)$ for $\Delta\varepsilon = 0.199$, $\Delta P = -0.25589$, $p = 0.38\text{GPa}$, $T_m = 228\text{K}$, $\theta_{sg} = -0.46918$, $T_{sg} = 121\text{K}$; 4. $\Delta\varepsilon_{lg}(\theta)$ for $\Delta\varepsilon = 0.104$, $\Delta P = -0.21549$, $p = 0.32\text{GPa}$, $T_m = 240\text{K}$, $\theta_{sg} = -0.43757$, $T_{sg} = 135\text{K}$; 5. At $T = T_{sg}$, the glass enthalpy coefficient is lowered by -0.37037 corresponding to the formation of an ultrastable polyamorphous phase after a constant volume change $\delta V = -0.224 \times 10^{-6} \text{m}^3/\text{g}$.

The ultrastable phase is stabilized under pressure at temperatures smaller than T_{sg} , and disappears far beyond T_{sg} , as shown in Figure 7. The glass transition temperatures of ultrastable phases are represented in Figure 7, and occur at temperatures extending from 131.5K for $p=0.55\text{GPa}$ to 150.5K for $p=0.32\text{GPa}$. The pressure contribution $\Delta P \times \Delta H_m$ disappears at T_g . These glass transitions are masked by crystallization.

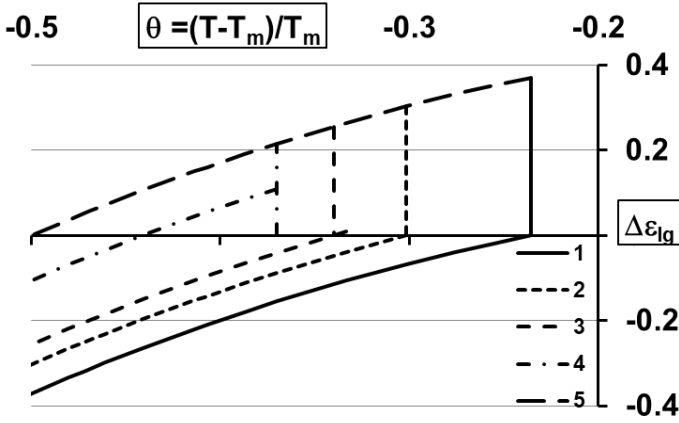


Figure 7: Calculated glass transition temperatures T_g of supercooled water under pressure p . The curves $\Delta\varepsilon_{lg}(\theta)$ numbered 1–4 complete those of Figure 6 at higher temperatures with $\Delta\varepsilon=0$: 1. $\Delta P=0.37037$, $p=0.55\text{GPa}$, $T_m=172\text{K}$, $\theta_g=-0.2357$, $T_g=131.5\text{K}$; 2. $\Delta P=0.30103$, $p=0.45\text{GPa}$, $T_m=210\text{K}$, $\theta_g=-0.3015$, $T_g=146.6\text{K}$; 3. $\Delta P=0.25589$, $p=0.38\text{GPa}$, $T_m=228\text{K}$, $\theta_g=-0.34009$, $T_g=150.5\text{K}$; 4. $\Delta P=0.21549$, $p=0.32\text{GPa}$, $T_m=240\text{K}$, $\theta_g=-0.37$, $T_g=150.5\text{K}$; 5- $\Delta\varepsilon=0$, $P_1-P_2=0$ (no volume change). The jumps of $\Delta\varepsilon_{lg}$ at θ_g are equal to ΔP with $\Delta\varepsilon=0$.

3. The phase diagram of supercooled water

The LLPT is announced by a specific heat increase extending from T_m at zero pressure down to 237K, and a specific heat peak under Laplace pressure of 0.31GPa down to 227.5K. This phenomenon characterizes the high specific heat increase observed many times in fragile glasses undergoing a first-order glass transition [30]. The line $\theta_{LL}=-0.167$ of these first-order transitions extends from $P=0$ to $P=0.8505$. The lines of homogeneous nucleation temperatures θ_1 and θ_2 of Phase 1 and Phase 2 in Figure 8 are calculated using (11–14) in the fragile state above $\theta_{LL}=-0.167$, with: $\varepsilon_{ls0}=1.8482$, $\varepsilon_{gs0}=1.586$, $P_1=P_2=P$, and in the strong state below θ_{LL} with (2,3,5,7), $\varepsilon_{ls0}=1.14286$, $\theta_{0m}^2=4/9$, $\varepsilon_{gs0}=0.66667$, $\theta_{0g}^2=1$, $P_1=P_2=P$, and P varying from 0 to 1.333. The value $P=1.333$ corresponds to the highest nucleation temperature $\theta_2=0$ of strong water in the absence of LLPT and to a pressure of about 0.6GPa for $V_m=0.74\times 18\times 10^{-6}\text{m}^3/\text{g}$. Two other lines, θ_{11} and θ_{22} , represented in the fragile state, are calculated assuming that the specific heat increase is not due to a virtual first-order glass transition at $\theta_g=-0.276$ but to a first-order transition occurring at $\theta_{LL}=-0.167$. In these conditions, the fragile water would undergo a virtual specific heat jump of $\Delta C_p=1.5\times \Delta H_m/T_m=33\text{J/mole}$ at $\theta_g=-0.2047$ in the absence of LLPT. In the two assumptions, the supercooled fragile water is homogeneous for $P > 0.4275$. It undergoes a first-order transition to Phase 1 and Phase 2 at θ_{LL} between the two critical points separating in Figure 8, the homogeneous regions in the fragile state from Phase 1 and Phase 2 in the strong state. The first one occurs here at $\theta_{LL}=-0.167$, $P=0.4275$, $p=0.152\text{GPa}$ if $V_m=16.8\times 10^{-6}\text{m}^3$. The second one occurs at $\theta_{LL}=-0.167$, $P=0.8505$, $p=0.31\text{GPa}$ if $V_m=16.5\times 10^{-6}\text{m}^3$. The existence of a first-order transition line has been already predicted by numerical simulation without introducing enthalpy difference between Phase 1 and Phase 2 [22,25,27,28]. The undercooled water is homogeneous in the strong state outside the area surrounded by Lines 1 and 2 for $P > 0.8505$ and $0 < P < 0.4275$. The transitions to Phase 3 below $\theta=-0.5$ are not represented because they involve a volume change, $V_1-V_2=\delta V$.

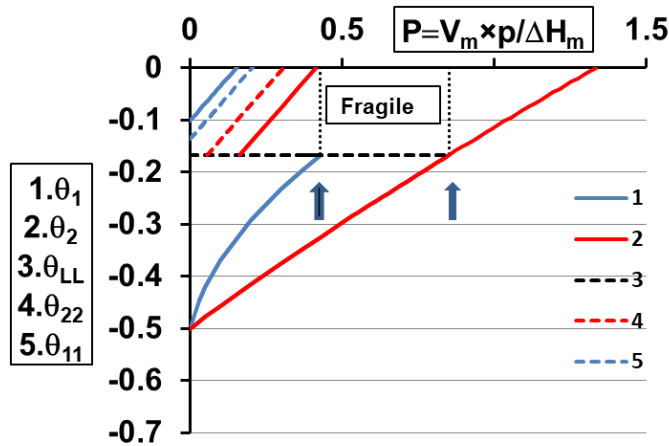


Figure 8 : Phase diagram of supercooled water at pressure p . Curves numbered from 1 to 5: 1. Homogeneous nucleation temperature of Phase 1 versus the enthalpy coefficient P induced by the pressure p above and below the LLPT; 2. Homogeneous nucleation temperature of Phase 2 versus the enthalpy coefficient P induced by the pressure p above and below the LLPT; 3. LLPT line separating the fragile liquid phase from the strong one at $\theta_{LL} = -0.167$; First critical point: $P = 0.4275$, $\theta = -0.16715$, $p = 0.152$ GPa if $V_m = 16.8 \times 10^{-6} \text{ m}^3$; Second critical point: $P = 0.8505$, $\theta = -0.16715$, $p = 0.33$ GPa if $V_m = 15.5 \times 10^{-6} \text{ m}^3$; 4. θ_{22} calculated assuming that the LLPT is not due to a fragile-to-strong transition; 5. θ_{11} calculated assuming that the LLPT is not due to a fragile-to-strong transition. Separation of Phase 1 and Phase 2 below LLPT line and between Lines 1 and 2. Homogeneous liquid in 2 regions: below θ_{LL} - from the first critical point to $P = 0$ and above Line 1; above the second critical point and below Line 2. Glass transitions giving rise to Phase 3 are not indicated.

Conclusion:

The thermodynamic parameters of the two water phases, Phase 1 and Phase 2, separated by an enthalpy saving depending on $\theta^2 = (T - T_m)^2 / T_m^2$, have been determined successfully only knowing the formation temperature of a strong glass in Phase 3 at $T_g = 136.6$ K, its melting heat, and its melting temperature. Supercooled water is a fragile liquid above a first-order liquid-to-liquid transition (LLPT) at $T_{LL} = 227.5$ K that is transformed into a strong liquid below T_{LL} . The LDA phase of the strong glass contains an enthalpy excess that increases its density to a value close to that of ice. The sharp transition temperatures T_{sg} under zero pressure, and the associated latent heats and volume changes, are calculated in good agreement with experimental results. The enthalpy excess presence in this bulk glass leads, at a transformation temperature T_{sg} , to the thermodynamic equilibrium of vitreous Phase 3 that is expected to be attained after years of relaxation.

Double glass transitions are predicted under pressure. The first-order glass-to-glass transitions under pressure, leading to high density amorphous phases called HDA and VHDA, result from the formation at temperatures T_{sg} of ultrastable polyamorphous states under pressure. The reduced glass transition temperature θ_g increases under pressure.

REFERENCES

1. R.F. Tournier. *Chem. Phys. Lett.* 665 (2016) 64.
2. K.L. Kearns, K.R. Whitaker, M.D. Ediger, H. Huth, and C. Schick, *J. Chem. Phys.* 2010, 133 (2010), 014702.
3. S. Singh, M.D. Ediger, and J.J. de Pablo. *Nature Materials.* 12 (2013), 139.
4. K. Ishii, and H. Nakayama, *Phys. Chem. Chem. Phys.* 16 (2014), 12073.
5. R.F. Tournier, *Chem. Phys. Lett.* 641 (2015), 9.
6. O. Mishima, *Proc. Jap. Acad. Sci. B, Phys. Biol. Sci.* 86 (2010), 165.
7. T. Loerting, and N. Giovambattista,. Amorphous ice. *J. Phys.: Condens. Matter*, 18 (2006), R919.
8. O. Mishima. *Nature.* 384 (1996), 546.
9. O. Mishima, *J. Chem. Phys.* 100 (1994), 5910.
10. O. Mishima, L.D. Calvert & E. Whalley, *Nature*, 314 (1985), 76.
11. O. Mishima, L.D. Calvert, & E. Whalley. *Nature.* 340 (1984), 393.
12. T. Loerting, V.V. Brazhkin, T. Morishita. *Adv. Chem. Phys.* 143 (2009), 29.
13. W. Kauzmann, *Chem. Rev.* 43 (1948), 219.
14. C.A. Angell, M. Oguni, and W.J. Sichina, *J. Phys. Chem.* 86 (1982), 998.
15. C.A. Angell, *Chem. Rev.* 2002, 102 (2002), 2627.
16. J.A. McMillan and S.C. Los. *Nature.* 206 (1965), 806.
17. M. Sugisaki, H. Suga, and S. Seki. *Bull. Chem. Soc. Jap.* 41 (1968), 2586.
18. K. Amann-Winkel, C. Gainaru, P.H. Handle, M. Seidt, H. Nelson, R. Böhmer, and T. Loerting, *PNAS.* 110 (2013), 17720.
19. M. Oguni, S. Maruyama, K. Wakabayashi, and A. Nagoe, *Chem. Asian J.* 2 (2007), 514.
20. S. Maruyama, K. Wakabayashi, and M. Oguni. *AIP Conf. Proc.* 706 (2004), 675.
21. D. Liu, Y. Zhang, C.-C. Chen, C.-Y. Mou, P.H. Poole, and S.-H. Chen. *PNAS.* 104 (2007), 9570.
22. P.H. Poole, F. Sciortino, U. Essmann & H.E. Stanley. *Nature.* 360 (1992), 324.
23. V. Holten, C.E. Bertrand, M.A. Anisimov, and J.V. Sengers, *J. Phys. Chem.* 136 (2012), 094507.
24. C.A. Angell, J. Shuppert, and J.C. Tucker,. *J. Phys. Chem.* 77, 26 (1971) 3092.

25. S.V. Buldyrev, M. Canpolat, S. Havlin, O. Mishima, M.R. Sadr-Lahijany, A. Scala, F.W. Starr and H. Stanley, *AIP Conf. Proc.* 469 (1999), 243.
26. K. Ito, C.T. Moynihan & C.A. Angell, *Nature*. 398 (1999), 492.
27. V. Holten & M.A. Anisimov, *Sci. Rep.* 2 (2012) ,713.
28. J.C. Palmer, F. Martelli, Y. Liu, R. Car, A.Z. Panagiotopoulos, P.G. Benedetti, *Nature*. 510 (2014), 385.
29. P.F. McMillan, *Roy. Soc. Chem.* 14 (2004), 1506.
30. R.F. Tournier, *Physica B.* 454 (2014), 253.
31. R.F. Tournier *Phys. B. Condens. Matter.* 392 (2007), 79.
32. R.F. Tournier, J. Bossy. *Chem. Phys. Lett.* 658 (2016), 282.
33. R.F. Tournier, *Chem. Phys. Lett.* 651 (2016) 198; Corrigendum, 675 (2017), 174.
34. D.Turnbull, *J. Chem. Phys.* 20 (1952), 411.
35. K. Lu, Y. Li. *Phys. Rev. Lett.* 80 (1998), 4474.
36. K. Winkel, E. Mayer, and T. Loerting. *J. Phys. Chem.* 115 (2011), 14141.
37. J.J Shephard and C.G Salzmann.. *J. Phys. Chem. Lett.* 7 (2016), 2281.
38. R.F. Tournier *Materials.* 4 (2011), 869.
39. R.F. Tournier, *Sci. Technol. Adv. Mater.* 10 (2009), 014501.
40. R.F. Tournier. *Rev. de Metall.* 109 (2012), 27.
41. R.J. Speedy and C.A. Angell. *J. Chem. Phys.* 65 (1976), 851.
42. R.A. Millero, F.J. Fine *J.Chem. Phys.* 59 (1973), 5529.
43. C.A. Angell, W.J. Sichina, M. Oguni. *J. Phys. Chem.* 86 (1982), 998.
44. D. Bertolini, M. Cassettari, and G. Salvetti. *Chem. Phys. Lett.* 199 (1985), 553.
45. E. Tombari, C. Ferrari, G. Salvelli, *Chem. Phys. Lett.* 300 (1999), 749.
46. I.K. Ishii, H. Nakayama, S. Hirabayashi, M. Nakayama., *Chem. Phys. Lett.* 459 (2008), 109.

..